Thermally Stable and Tunable Broadband Near-infrared Emission from NIR-I to NIR-II Based in Bi-doped Germanate Glass for Smart Light Source

Weiwei Chen [a], Xiongjian Huang [a, b], Quan Dong [a], Zhihao Zhou [a], Puxian Xiong [b], Yakun Le [a], Enhai Song [a], Jianrong Qiu [c], Zhongmin Yang [a, b],and Guoping Dong* [a]

[a] *The State Key Laboratory of Luminescent Materials and Devices, and Guangdong Engineering Technology Research and Development Center of Special Optical Fiber Materials and Devices, and Guangdong Provincial Key Laboratory of Fiber Laser Materials and Applied Techniques, School of Materials Science and Engineering, South China University of Technology, Guangzhou 510641, P. R. China*

[b] *School of Physics and Optoelectronic, Guangdong Provincial Key Laboratory of Fiber Laser Materials and Applied Techniques, Guangdong Engineering Technology Research and Development Center of Special Optical Fiber Materials and Devices, The State Key Laboratory of Luminescent Materials and Devices, South China University of Technology, Guangzhou 510640, China.*

[c] *State Key Laboratory of Modern Optical Instrumentation, College of Optical Science and Engineering, Zhejiang University, Hangzhou 310027, P. R. China*

Corresponding authors.

E-mail addresses: dgp@scut.edu.cn *(G.P. Dong)*

Contents

Supplementary Figures

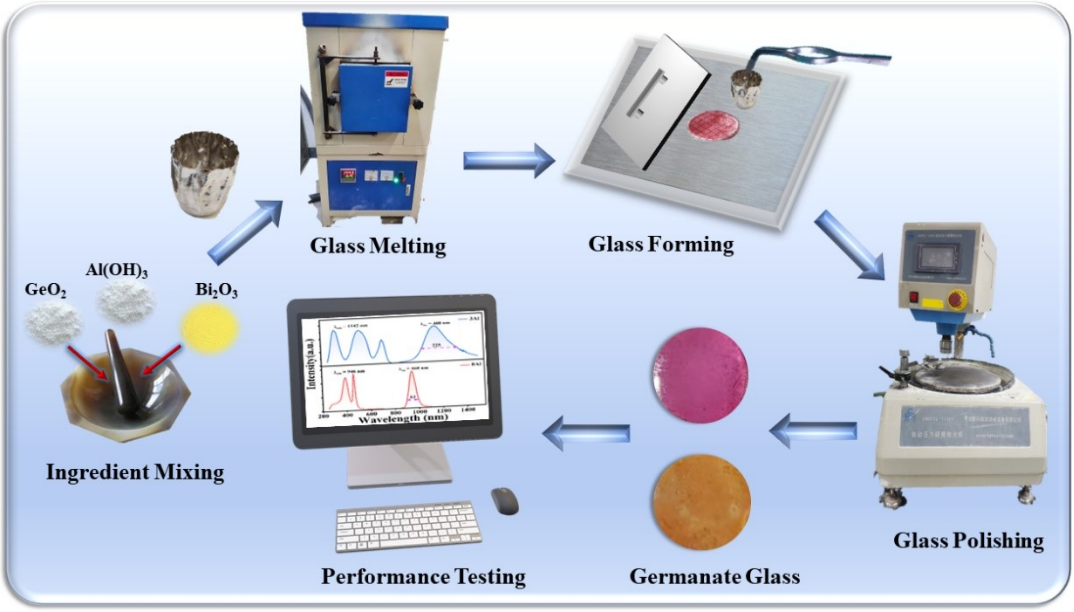

Fig. S1 Schematic diagram of germanate glass melting process.

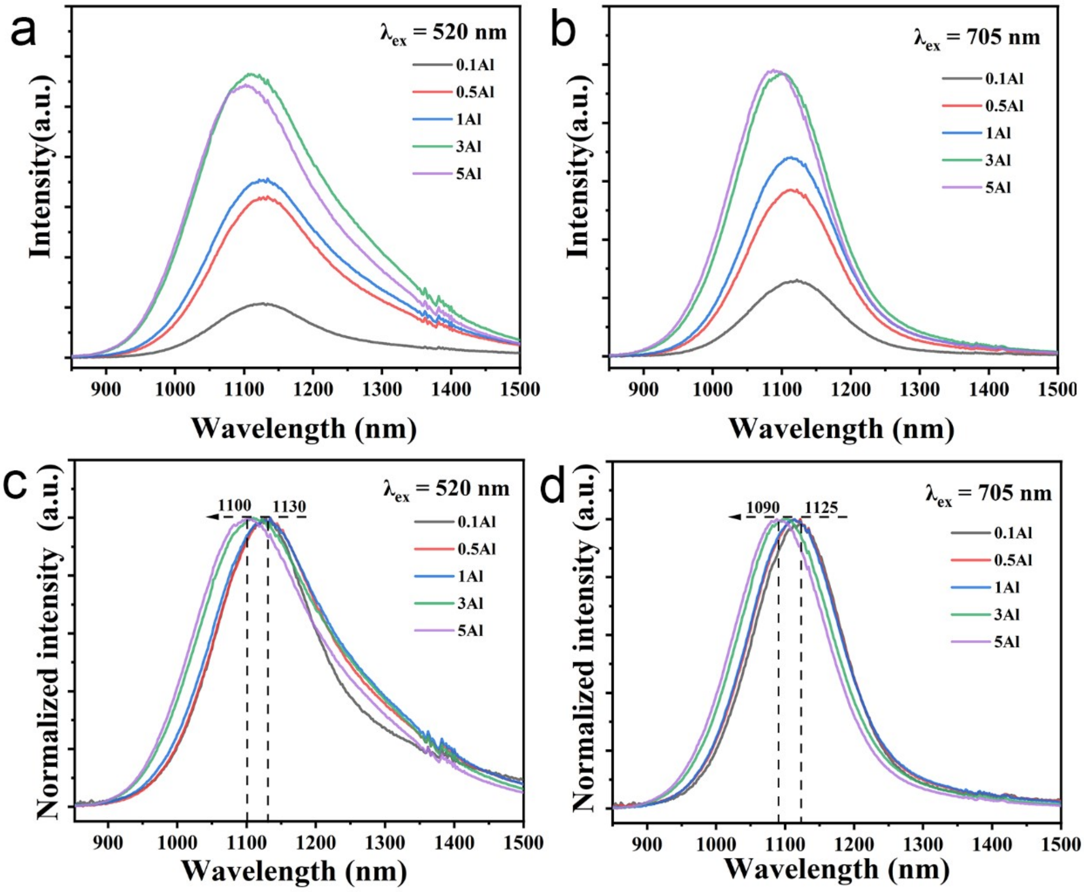

Fig. S2 Emission spectra of Bi-doped germanate glasses with different Al_2O_3 content under various excitation wavelength (a) λ_{ex} = 520 nm and (b) λ_{ex} = 705 nm. (c), (d) Corresponding normalized emission spectra of (a) and (b).

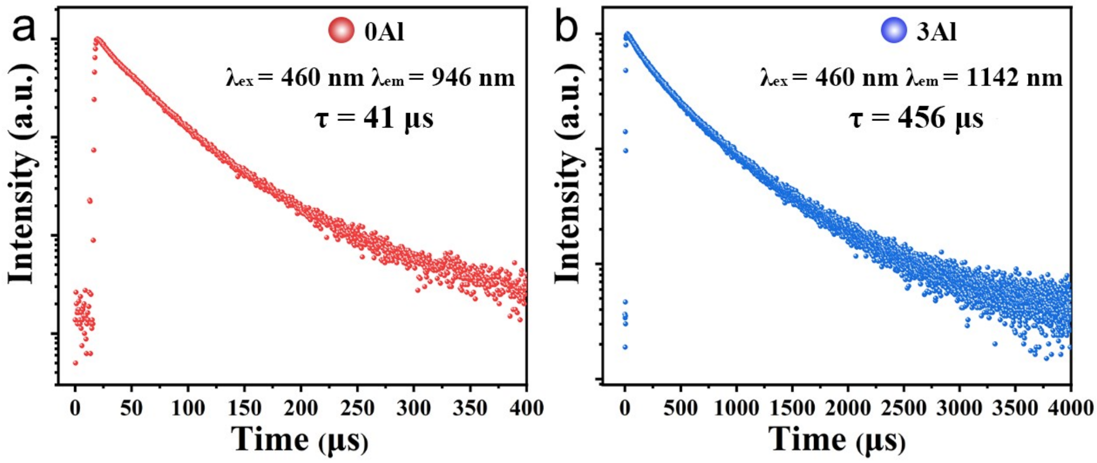

Fig. S3 Emission lifetime of (a) 0Al and (b) 3Al sample.

The effective fluorescence lifetime τ is evaluated through the following equation[S1]:

$$\tau = \int I(t)tdt \,/ \int I(t)dt \tag{1}$$

where *I(t)* represents the emission intensity *I* at time *t*. Under excitation at 460 nm, the obtained lifetimes for the individual emission bands at 946 and 1142 nm of 0Al and 3Al sample are 41 and 456 μs, respectively.

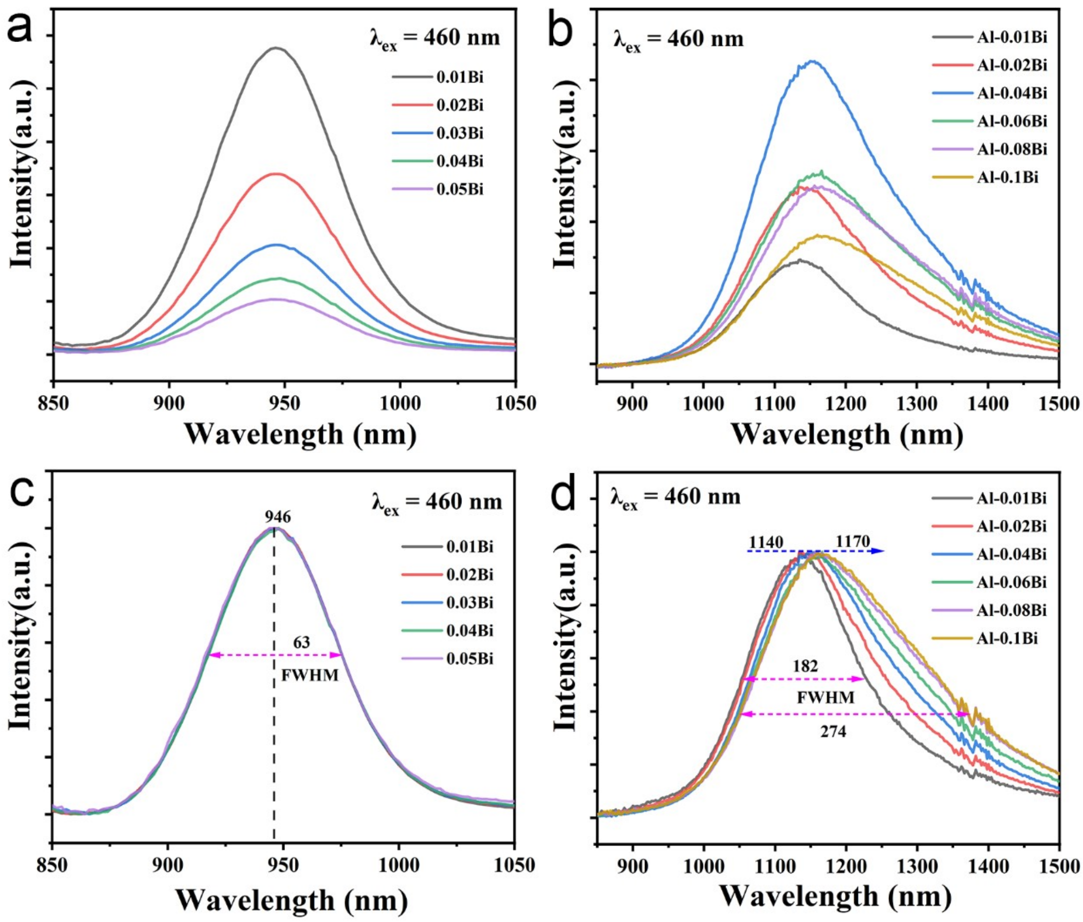

Fig. S4 Emission spectra (λ_{ex} = 460 nm) of (a) (100-y)GeO_2-yBi_2O_3 (yBi, y =0.01, 0.02, 0.03, 0.04, 0.05, in mol%) and (b) (97-z)GeO_2-3Al_2O_3-zBi_2O_3 (Al-zBi, z =0, 0.01, 0.02, 0.04, 0.06, 0.08, 0.1, in mol%) samples. (c), (d) Corresponding normalized emission spectra of (c) and (d).

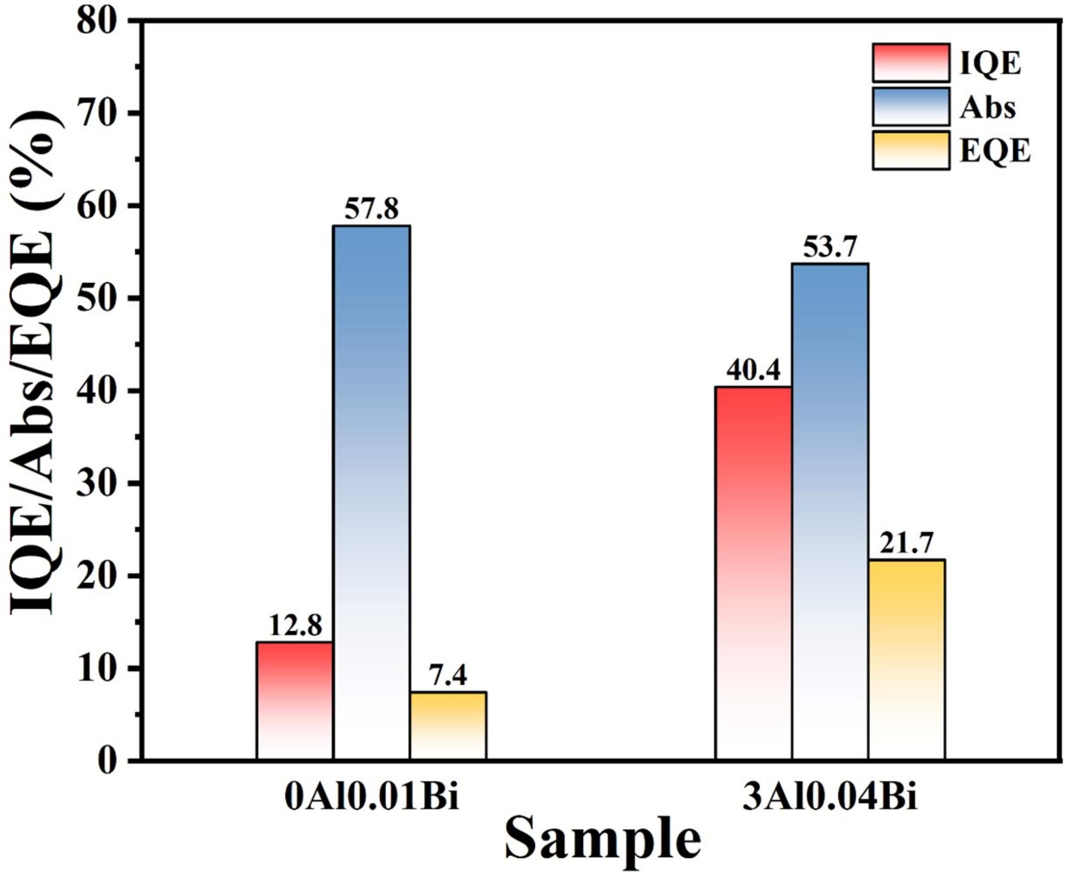

Fig. S5 The internal/external quantum efficiency (IQE, EQE) and absorption efficiency (Abs) of 0.01Bi and Al-0.04Bi sample (λ_{ex} = 460 nm).

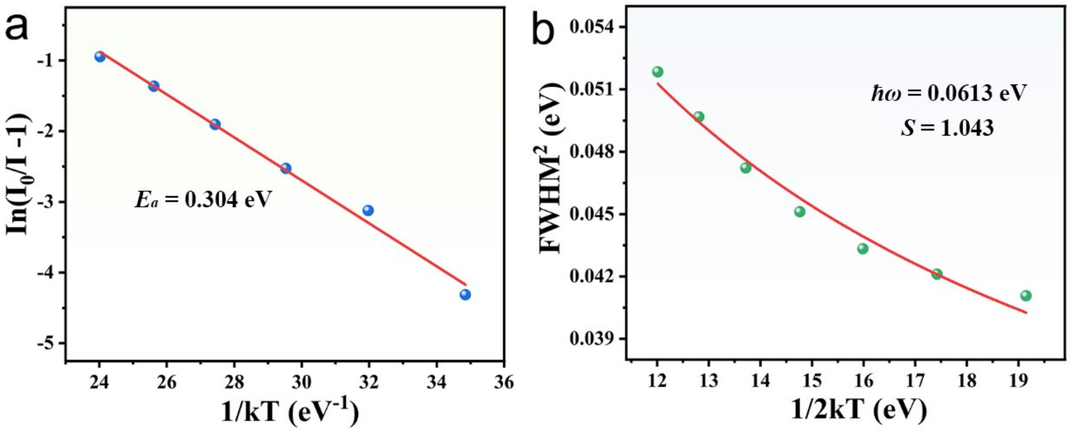

Fig. S6 (a) Plotting of ln[(I_0/I) −1] versus 1/(kT) of Al-0.04Bi sample. (b) Fitting results of square of full width at half maximum (FWHM^2) as a function of 1/2kT.

The Arrhenius equation is: [S2]

$$I_T = \frac{I_0}{1 + A\exp(-\frac{E_a}{kT})} \tag{2}$$

where I_T and I_0 are the integrated intensity at certain temperature and RT, respectively; A represents a constant; k stands for the Boltzmann constant (8.617×10^{-5} eV K^{-1}). The corresponding E_a is the activation energy for thermal quenching. It was obtained as the slope of plotting of ln[(I_0/I_T) − 1] versus 1/(kT) and equals to 0.304 eV.

The Huang–Rhys factor (S) can reflect how strongly electrons couple to phonons and can be obtained by fitting the temperature-dependent full width at FWHM of photoluminescence peaks using the following equation: [S5, S7]

$$FWHM = 2.36\sqrt{S}\hbar\omega\sqrt{\coth(\frac{\hbar\omega}{2kT})} \tag{3}$$

and by simplifying, we can figure out

$$FWHM^2 = a + \frac{b}{1/2kT} \tag{4}$$

where the $\hbar\omega$ and k are the mean phonon energy and Boltzmann's constant, a = 5.57 × S × ($\hbar\omega$)^2 and b = 5.57 × S × ($\hbar\omega$) S^2. The values of $\hbar\omega$ and S are 0.0613 eV and 1.043, respectively.

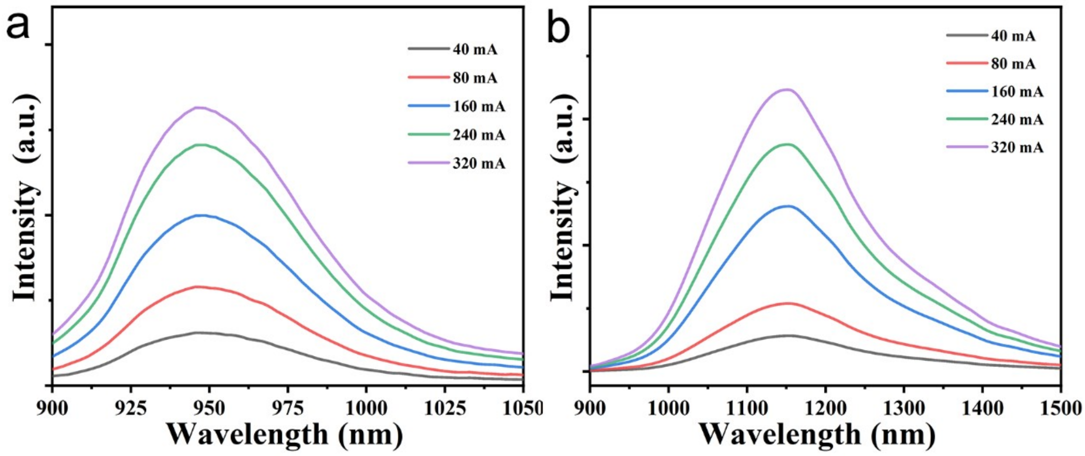

Fig. S7 Driven current-dependent emission spectra of the fabricated NIR LED based on (a) 0.01Bi (NIR-LED-I) and (b) Al-0.04Bi (NIR-LED-II) sample measured by a portable fiber spectrometer (NIRQUEST 512, Ocean Optics, NIR, 900-1700 nm).

Supplementary Table

Table S1 Performance comparison of Bi-doped high germanate glass developed here with the reported broadband NIR phosphors, glasses and glass ceramics. λ_{ex} represents the excitation wavelength, λ_{em} represents the peak emission wavelength and $I_{150°C}$ is the retained emission intensity when the temperature is increased from room temperature to 150 °C.

Composition	λ_{ex} (nm)	λ_{em} (nm)	FWHM (nm)	$I_{150°C}$ (%)	Device performance	Ref.
$K_3LuSi_2O_7:Eu^{2+}$	460	740	160	59	25.1 mW @ 120 mA	S3
$YCAS:Cr^{3+}$	440	760	160	90.1	62.6 mW@ 100 mA	S4
$K_2NaScF_6:Cr^{3+}$	435	765	101	89.6	393.7 mW@ 300 mA	S5
$K_3ScF_6:Cr^{3+}$	432	770	150	87.3	139.6 mW@ 600 mA	S6
$Cs_2KGaF_6:Cr^{3+}$	439	782	110	88.7	183.8 mW @ 320 mA	S7
$Ca_2LuHf_2Al_3O_{12}:Cr^{3+}$	460	785	145	65	46.1 mW@ 100 mA	S8
$KAlP_2O_7:Cr^{3+}$	450	790	120	77	80.9 mW@ 350 mA	S9
$CaLuScGa_2Ge_2O_{12}:Cr^{3+}$	465	800	150	59	1.2 mW@ 100 mA	S10
$MgAl_2O_4:Mn^{2+}$	450	813	125	40	78.4 mW@ 120 mA	S11
$LiInSi_2O_6:Cr^{3+}$	460	840	143	77	51.6 mW@ 100 mA	S12
Te doped borate glass	435	904	240	-	31.6 mW@ 800 mA	S13
$MgO:Cr^{3+}, Ni^{2+}$	455	1335	235	83	27.4 mW@ 300 mA	S14
$LiMgPO_4:Cr^{3+}, Ni^{2+}$	450	1380	273	45	2.7 mW@ 120 mA	S15
$Y_3Al_2Ga_3O_{12}:Ni^{2+}$	400	1450	300	71	1.3 mW@ 300 mA	S16
Bi doped germanate glass	460	946	63	84	21.3 mW@ 160 mA	This work
					53.2 mW@ 320 mA	
		1142	225	87	90.7 mW@ 160 mA	
					179.5 mW@ 320 mA	

Supplementary References

1. J. Cao, S. Xu, Q. Zhang, Z. Yang and M. Peng, *Adv Opt Mater*, 2018, **6**, 1801059.
2. X. Zhou, W. Geng, J. Li, Y. Wang, J. Ding and Y. Wang, *Adv Opt Mater*, 2020, **8**, 1902003.
3. J. Qiao, G. Zhou, Y. Zhou, Q. Zhang and Z. Xia, *Nat Commun*, 2019, **10**, 5267.
4. G. Zheng, W. Xiao, J. Wu, X. Liu, H. Masai and J. Qiu, *Adv Sci (Weinh)*, 2022, **9**, e2105713.
5. E. Song, H. Ming, Y. Zhou, F. He, J. Wu, Z. Xia and Q. Zhang, *Laser Photonics Rev*, 2020, **15**, 2000410.
6. H. J. Yu, J. Chen, R. Y. Mi, J. Y. Yang and Y. G. Liu, *Chem Eng J*, 2021, **417**, 129271.
7. Z. X. Wu, X. X. Han, J. Wang, Y. Y. Zhou, K. Xing, S. Cao, J. L. Zhao, B. S. Zou and R. S. Zeng, *J Mater Chem C*, 2022, **10**, 10292-10301.
8. L. Zhang, D. Wang, Z. Hao, X. Zhang, G.-h. Pan, H. Wu and J. Zhang, *Adv Opt Mater*, 2019, **7**, 1900185.
9. H. Zhang, J. Zhong, F. Du, L. Chen, X. Zhang, Z. Mu and W. Zhao, *ACS Appl Mater Inter*, 2022, **14**, 11663-11671.
10. B. Bai, P. Dang, D. Huang, H. Lian and J. Lin, *Inorg Chem*, 2020, **59**, 13481-13488.
11. E. Song, X. Jiang, Y. Zhou, Z. Lin, S. Ye, Z. Xia and Q. Zhang, *Adv Opt Mater*, 2019, **7**, 1901105.
12. X. X. Xu, Q. Y. Shao, L. Q. Yao, Y. Dong and J. Q. Jiang, *Chem Eng J*, 2020, **383**, 123108.
13. L. L. Tan, Y. Q. Fu, S. L. Kang, L. Wondraczek, C. G. Lin and Y. Z. Yue, *Photonics Res*, 2022, **10**, 1187-1193.
14. B.-M. Liu, X.-X. Guo, L.-Y. Cao, L. Huang, R. Zou, Z. Zhou and J. Wang, *Chem Eng J*, 2023, **452**, 139313.
15. S. H. Miao, Y. J. Liang, Y. Zhang, D. X. Chen and X. J. Wang, *Adv Mater Technol-Us*, 2022, 2200320, DOI: 10.1002/admt.202200320.
16. L. Yuan, Y. Jin, H. Wu, K. Deng, B. Qu, L. Chen, Y. Hu and R.-S. Liu, *ACS Appl Mater Inter*, 2022, **14**, 4265-4275.